

Strasbourg, 23rd. January 2008

NUMERICAL SIMULATION OF LASER-INDUCED CAVITATION BUBBLES

Mathieu Bachmann

Institut für Geometrie und Praktische Mathematik,
RWTH Aachen

Joint work with :

Josef Ballmann, Siegfried Müller, *RWTH Aachen*.

Dennis Kröninger, Thomas Kurz, *Universität Göttingen*.

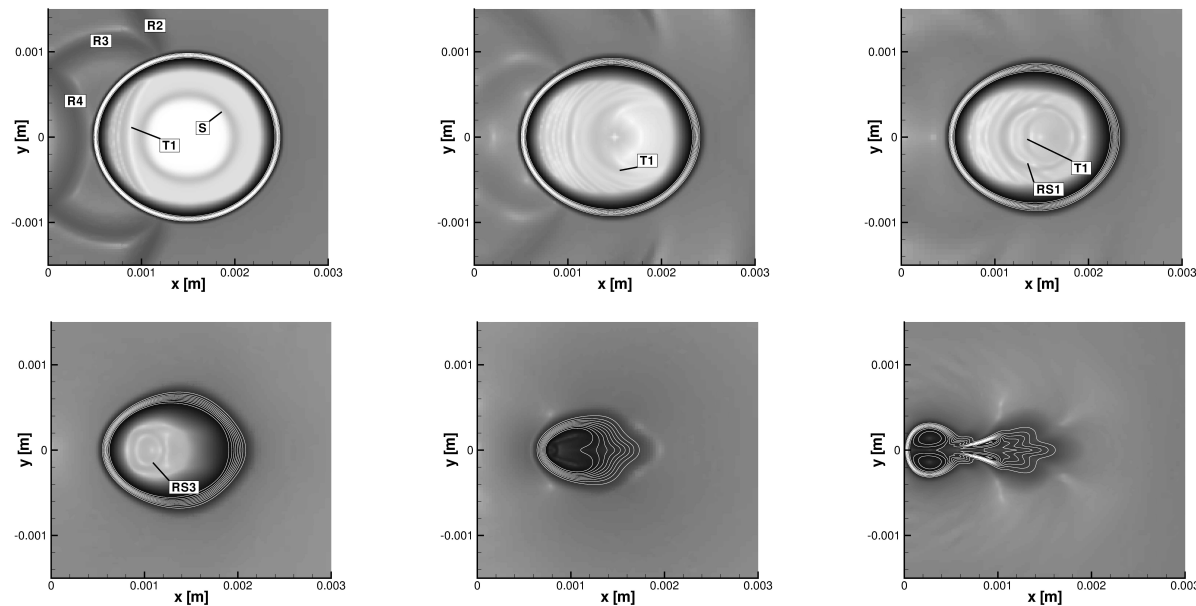
Philippe Helluy, Hélène Mathis, *Université de Louis Pasteur Strasbourg*.

Outline

1. Introduction
2. Experiments
3. Mathematical Model
4. Discretization
5. Initial data
6. Numerical simulation and validation
7. Conclusion and Outlook

Introduction

- **Goal** : Investigation of flow phenomena caused by a collapsing bubble.

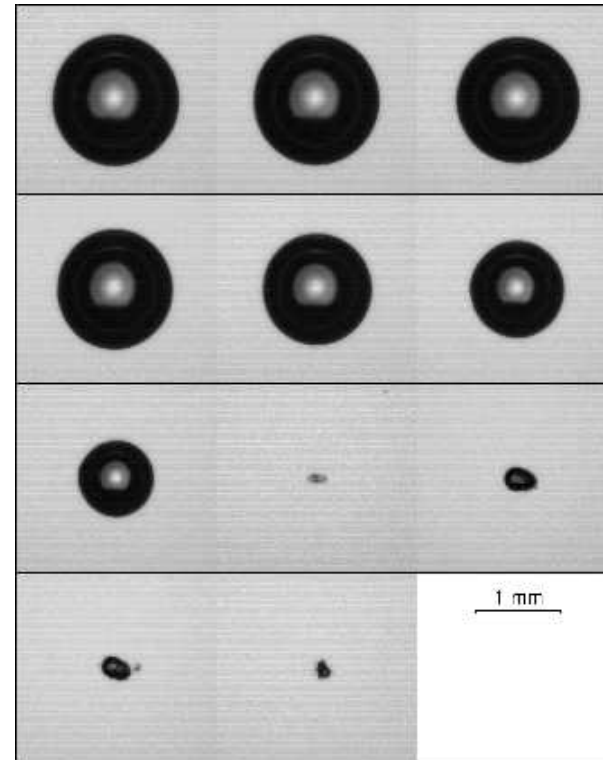


- **Need**: Mathematical model + Initial data

⇒ Focus on the modelling and the simulation of a single bubble.

Experiments

- Bubbles induced by laser pulses in a container of size $50 \times 50 \times 50 \text{ mm}^3$.
- $R_{max} = 1 \text{ mm}$.
- $R_{min} = 10 \mu\text{m}$.
- The experiment last $200 \mu\text{s}$.



Mathematical Model

- The 1d-Euler equations in spherical coordinates

$$\begin{aligned} \frac{\partial}{\partial t}(r^2 \rho) + \frac{\partial}{\partial r}(r^2(\rho v_r)) &= 0 \\ \frac{\partial}{\partial t}(r^2 \rho v_r) + \frac{\partial}{\partial r}(r^2(\rho v_r^2 + p)) &= 2 p r \\ \frac{\partial}{\partial t}(r^2 \rho E) + \frac{\partial}{\partial r}(r^2(\rho v_r(E + p/\rho))) &= 0 \end{aligned} \quad (1)$$

- The stiffened gas pressure law is used to close the system.

$$p(\rho, e, \varphi) = (\gamma(\varphi) - 1)\rho e - \gamma(\varphi)\pi(\varphi). \quad (2)$$

φ is the phase indicator function (gas fraction, level set function).

Saurel Abgrall Approach

- The two phases (gas and liquid) are distinguished by the mass fraction φ which satisfies a transport equation without mass transfer.

$$\frac{\partial \varphi}{\partial t} + v_r \frac{\partial \varphi}{\partial r} = 0.$$

- For the pure phases, the coefficients γ and π are obtained by measurements.
- A linear interpolation between the two phases is used for the mixture,

$$\beta_1(\varphi) = \varphi\beta_1(1) + (1 - \varphi)\beta_1(0),$$

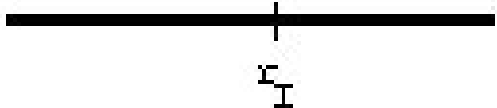
$$\beta_2(\varphi) = \varphi\beta_2(1) + (1 - \varphi)\beta_2(0).$$

where β_1 and β_2 are defined by $\beta_1 = 1/(\gamma - 1)$ and $\beta_2 = \gamma\pi/(\gamma - 1)$. 6

Level Set Method

- This approach represents the interface as a zero level set of a smooth function ϕ which is the signed distance from the interface.

$$\phi(r, t) = \begin{cases} r_I - r, & r < r_I \\ 0, & r = r_I \\ r - r_I, & r > r_I \end{cases}$$



- The evolution of this function ϕ is governed by a transport equation,

$$\frac{\partial \phi}{\partial t} + v_r \frac{\partial \phi}{\partial r} = 0 \quad \text{with} \quad \left| \frac{\partial \phi}{\partial r} \right| = 1.$$

- The level set is reinitialized to keep ϕ a distance function,

$$\frac{\partial \tilde{\phi}}{\partial \tau} = S(\tilde{\phi}) \left(1 - \left| \frac{\partial \tilde{\phi}}{\partial r} \right| \right) \quad S(\tilde{\phi}) = \begin{cases} -1, & \tilde{\phi} < 0 \\ 0, & \tilde{\phi} = 0 \\ 1, & \tilde{\phi} > 0 \end{cases} \quad 7$$

Discretization Fluid Equations

- The Euler equations are solved by a finite volume scheme

$$\mathbf{v}_i^{n+1} = \mathbf{v}_i^n - \frac{\Delta t}{\Delta r_i^3} \left(r_{i+\frac{1}{2}}^2 \mathbf{F}_{i+\frac{1}{2}}^{n,-} - r_{i-\frac{1}{2}}^2 \mathbf{F}_{i-\frac{1}{2}}^{n,+} \right) + \frac{\Delta r_i \Delta t}{\Delta r_i^3} \mathbf{S}_i^n$$

with

$$\mathbf{v} = (\rho, \rho v_r, \rho E)^T,$$

$$\Delta r_i := r_{i+\frac{1}{2}} - r_{i-\frac{1}{2}}, \quad \Delta r_i^3 := \frac{1}{3} \left(r_{i+\frac{1}{2}}^3 - r_{i-\frac{1}{2}}^3 \right), \quad \hat{r}_i := \frac{1}{2} \left(r_{i+\frac{1}{2}} + r_{i-\frac{1}{2}} \right),$$

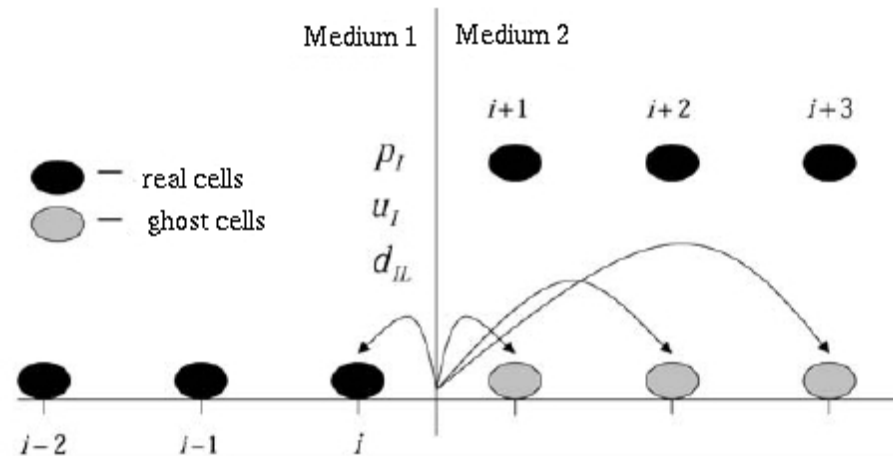
$$\mathbf{S}_i^n := (0, 2\hat{r}_i p_i^n, 0).$$

- Multiscale grid adaptation (Müller)

Numerical Flux: Saurel Abgrall Method

- Second order ENO reconstruction of primitive variables ρ, v_r, p, φ
- Exact Riemann solver for the flux
 - \Rightarrow 1D contact discontinuities are preserved

Numerical Flux: Real Ghost Fluid Method (Wang, Liu, Khoo)



- A Riemann problem is defined at the interface and solved for predicting the interfacial states (ρ_{IL} , ρ_{IR} , p_I and u_I).
- This state redefines the real fluid next to the interface and the ghost cells as boundary conditions.
- The solution can be advanced to the next time step.

Discretization : Indicator Function

- **Mass gas fraction:**
Upwind discretization (Saurel/Abgrall)

$$\varphi_i^{n+1} = \varphi_i^n - \frac{\Delta t}{\Delta r_i^3} \left(r_{i+\frac{1}{2}}^2 \bar{v}_{r,i+\frac{1}{2}}^n (\bar{\varphi}_{i+\frac{1}{2}}^n - \varphi_i^n) - r_{i-\frac{1}{2}}^2 \bar{v}_{r,i-\frac{1}{2}}^n (\bar{\varphi}_{i-\frac{1}{2}}^n - \varphi_i^n) \right)$$

- **Level set:**
First order time discretization and a second order upwind space discretization

Initial Data

- It's not possible to measure experimentally the state inside the bubble.
- It is possible to approximate the state inside the bubble from the equilibrium radius R_{eq} using the static equilibrium and the perfect gas law.

– At static equilibrium we have
$$p_i(R_{eq}) = p_0 + \frac{2\sigma}{R_{eq}}.$$

- The equilibrium radius R_{eq} is calculated from the Keller-Miksis model.

– With the adiabatic law, we obtain the pressure

$$p_i(R_b) = p_0 \left(\frac{R_{eq}^3}{R_b^3} \right)^\gamma$$

– With the adiabatic law we obtain the density

$$\rho_i(R_b) = \rho_0 \left(\frac{p_i(R_b)}{p_0} \right)^{1/\gamma}$$

- With $R_{eq} = 6.92 \times 10^{-5}$ m we compute the initial states,

	Initial data		Material parameters			
	ρ [kg/m ³]	p [Pa]	γ [-]	π [Pa]	c_v [J/kg K]	\mathcal{R} [J/kg K]
Gas	9.5e-4	4.57	1.4	0	708.3	283.32
Liquid	998	100000	1.1	2.e+9	4190.0	418

Keller-Miksis Model

- Model for liquid motion induced by a spherical cavity in an infinite medium.
- Incompressibility, sound radiation, the van der Waals gas law, ...

$$\left(1 - \frac{\dot{R}_b}{c}\right) R_b \ddot{R}_b + \frac{3}{2} \dot{R}_b^2 \left(1 - \frac{\dot{R}_b}{3c}\right) = \left(1 + \frac{\dot{R}_b}{c}\right) \frac{P_R - p_0}{\rho} + \frac{R_b d(P_R - p_0)}{\rho c dt}, \quad (3)$$

where P_R denotes the pressure at bubble radius R_b given by

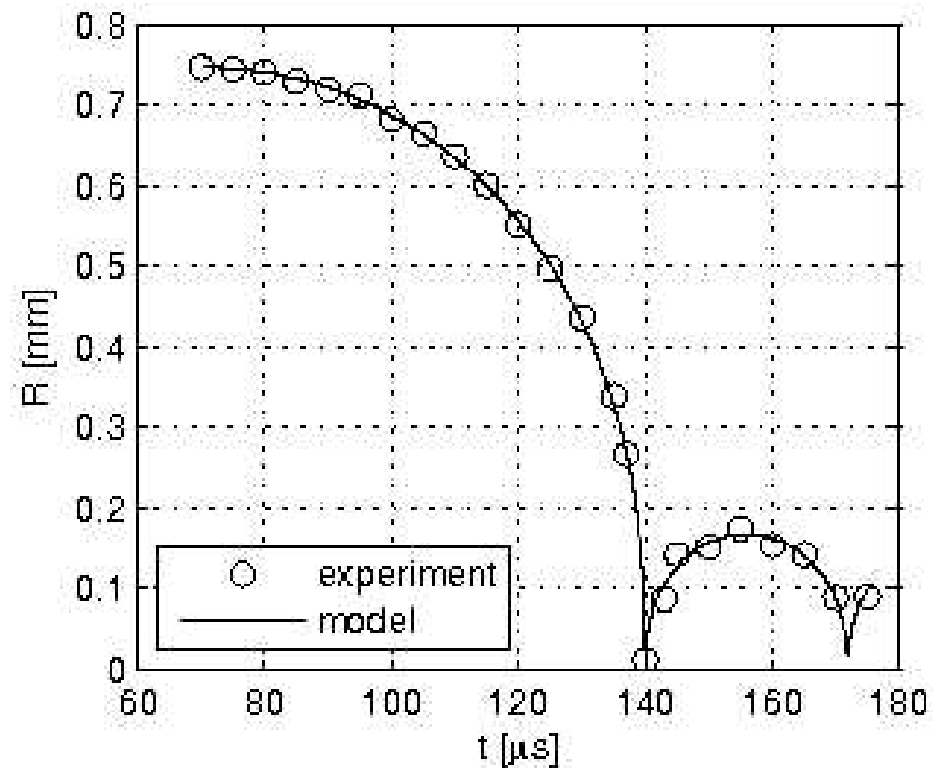
$$P_R = \left(p_0 - p_v + \frac{2\sigma}{R_{eq}}\right) \left(\frac{R_{eq}^3 - b R_0^3}{R_b^3 - b R_0^3}\right)^\gamma - \frac{2\sigma}{R_b} - \frac{4\mu\dot{R}_b}{R_b} + p_v. \quad (4)$$

Fitting of Equilibrium Radius

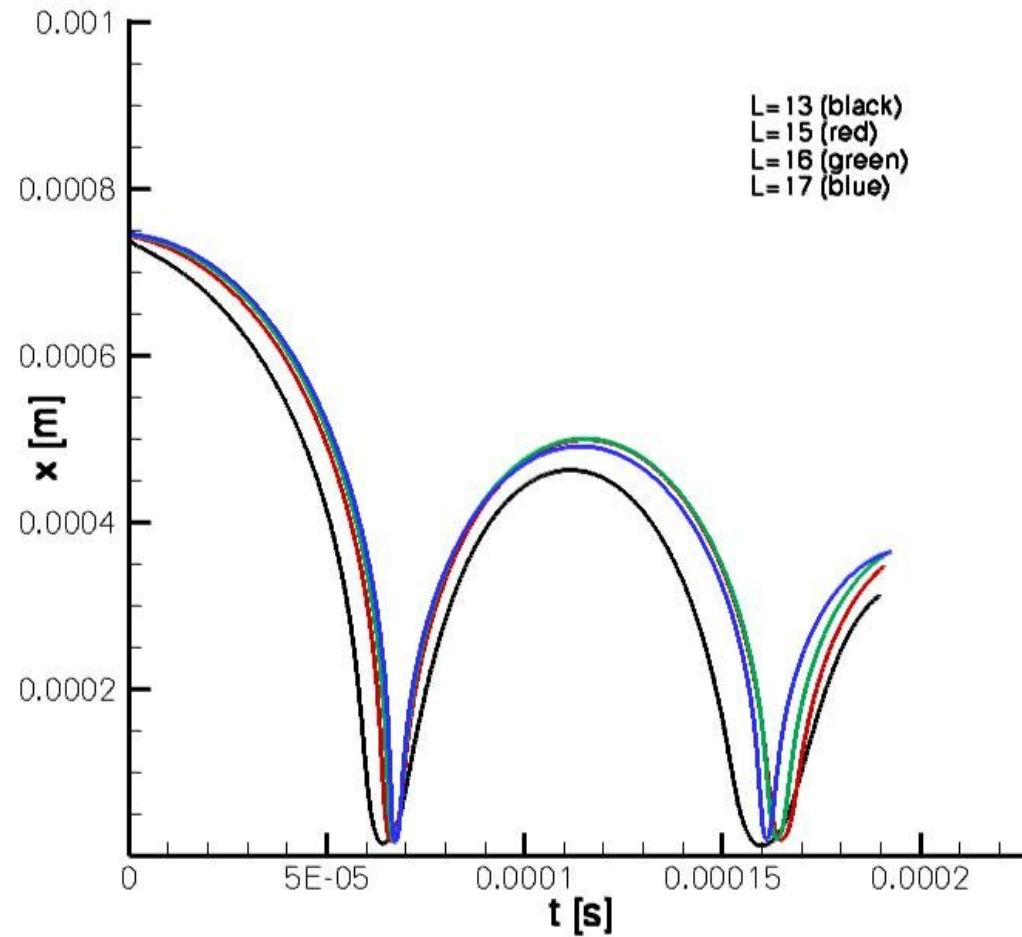
Initial conditions :

- $t_{max} = 70.7 \mu s$ ("Exp")
- $R_b = R_{max}$ (Exp)
- $\dot{R}_b = 0$

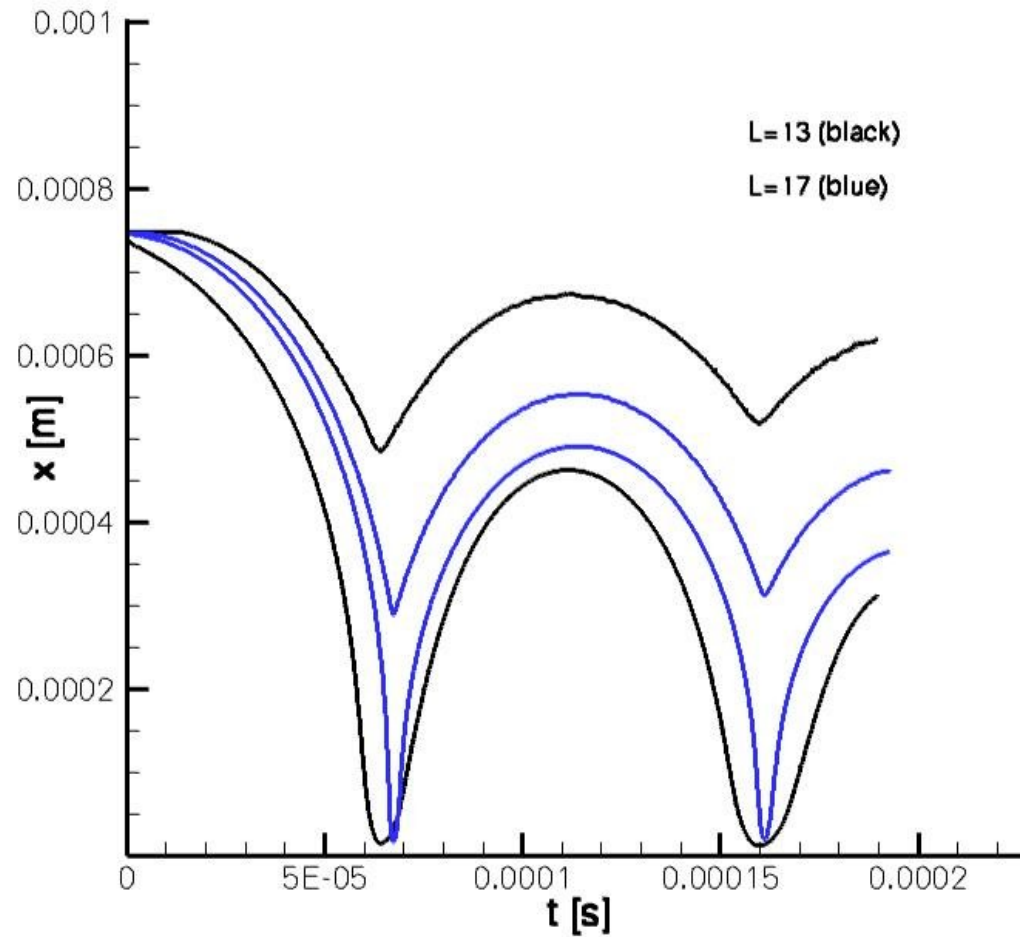
$\Rightarrow R_{eq} = 6.92 \times 10^{-5} \text{ m}$
in minimizing the least square error.



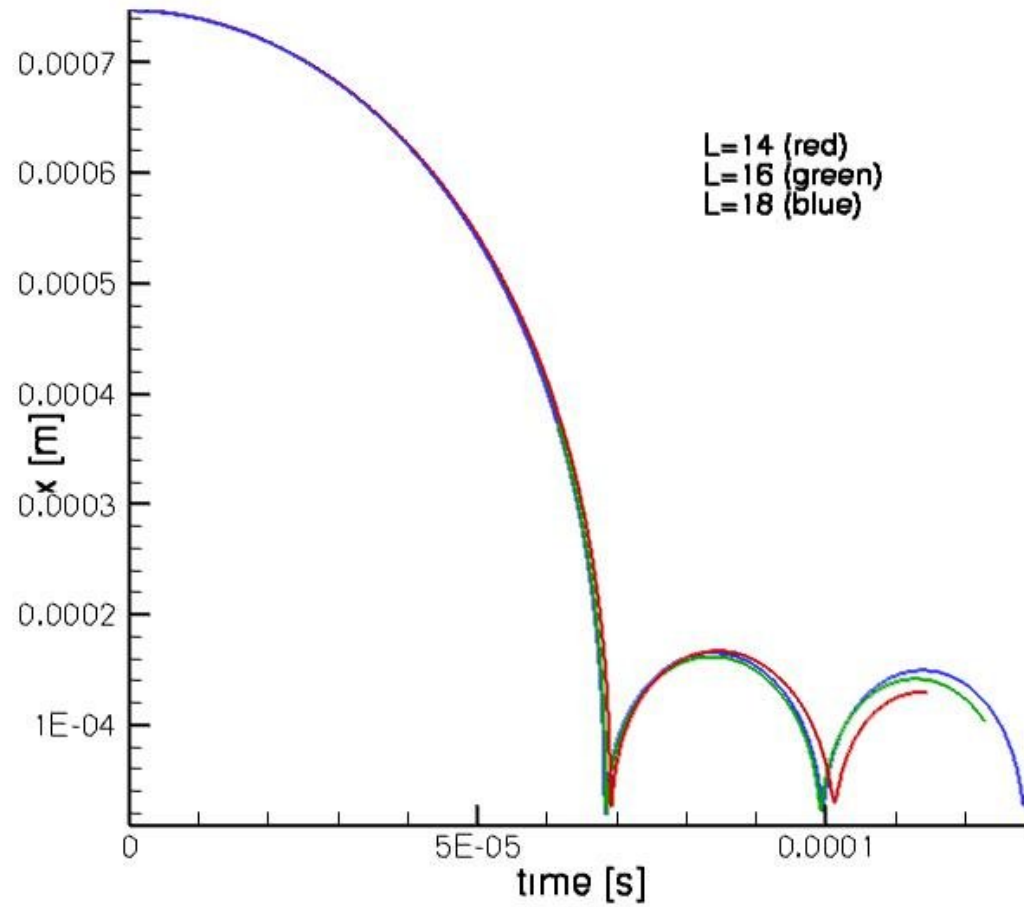
Numerical Results: Saurel-Abgrall Approach



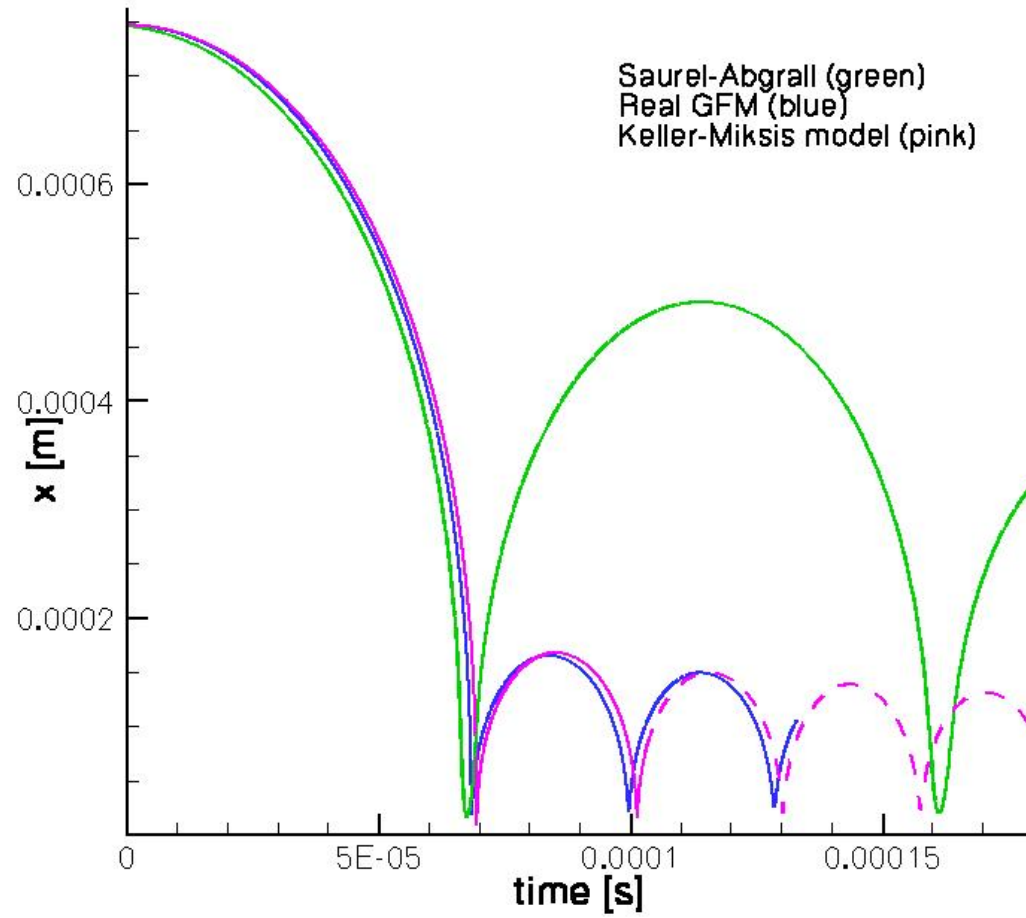
Numerical Results: Saurel-Abgrall Approach



Numerical Results: Real Ghost Fluid Method



Numerical Results: Validation



Numerical Results: Validation

Levels of refinement		Saurel-Abgrall Approach					Real Ghost Fluid Method			K-M Model
		L13	L14	L15	L16	L17	L14	L16	L18	
1st collapse	time [μs]	64.1	65.4	66.3	67.0	67.4	69.2	68.5	68.5	69.33
	radius [μm]	16.0	17.5	17.8	17.54	16.7	25.8	17.5	18.7	9.176
	pressure [$10^5 Pa$]	56.6	87.0	131	196	290	100.6	398	300	1510
1st rebound	time [μs]	111.5	114.3	115.4	115.2	113.9	84.5	83.6	83.7	85.8
	radius [μm]	462	487	500	500	491	166.6	161.6	165.17	167.8
	pressure [Pa]	0.97	4	7.6	11.8	17	3450	3226	3140	4348
2nd collapse	time [μs]	159.6	163.8	164.8	163.8	161.1	101.2	99.3	99.5	101.2
	radius [μm]	12.8	17.24	19.32	20.07	20.0	29.5	22.6	22	16.4
	pressure [$10^5 Pa$]	27	41	59	83	112	58	130	150	369

Conclusion

Saurel-Abgrall:

- Severe numerical phase transition
- Rebound overpredicted
- Slow grid convergence
- Shock strength underpredicted

Real Ghost Fluid Method:

- No phase transition
- Rebound well-predicted
- Slow grid convergence
- Shock strength underpredicted

Future Work

- Van der Waals + Real Ghost Fluid method
- 2D/3D implementation of the Real Ghost Fluid method
- Collapse near a wall and comparison with Saurel-Abgrall